UNIVERSIDAD NACIONAL DE COLOMBIA
SEDE MEDELLÍN
FACULTAD DE MINAS

DYNA
http://dyna.medellin.unal.edu.co/

Protection against corrosion by molten salts through aluminum coatings deposited by arc thermal spray on ASTM A53 grade B steel

Diego Pérez-Muñoz, José Luddey Marulanda-Arévalo & José Luis Tristancho-Reyes

Faculty of Mechanical Engineering, Universidad Tecnológica de Pereira, Pereira, Colombia. dperez@utp.edu.co, jlmarulanda@utp.edu.co, jostris@utp.edu.co

Received: July 8th, 2019. Received in revised form: February 6th, 2020. Accepted: February 28th, 2020

Abstract
ASTM A53 steel samples were coated with aluminum by EATS, they report continuity and adherence. Thermal treatment improved their performance against corrosion, because the aluminum inter-diffusions occur from coating into substrate and iron from substrate into coating. Samples were subjected to molten salt corrosion (20% Na_2SO_4 and 80% V_2O_5) in the temperature range of 400 °C-600 °C. Samples were characterized by SEM-EDS and the morphology of layers was studied, revealing good protection of the layer deposited, and the degradation of coating occurred above fusion temperatures of the salts. Moreover, the corrosion rate increased with temperature and decreased with exposition time.

Keywords: aluminium; corrosion; high temperature; thermal spray.

Protección contra la corrosión por sales fundidas del acero ASTM A53 grado B recubrimiento con aluminio depositado por rociado térmico por arco eléctrico

Resumen
Muestras del acero ASTM A53 grado B fueron recubiertas por rociado térmico por arco eléctrico con aluminio; estos recubrimientos presentan una buena continuidad y adherencia. Se les realizó un tratamiento térmico para mejorar su desempeño a la corrosión, ya que se produce la inter difusión del aluminio del recubrimiento hacia el substrato y del hierro del substrato hacia el recubrimiento. Luego fueron sometidas a corrosión por sales fundidas compuestas por 20 % de sulfato de sodio (Na_2SO_4) y 80 % de pentóxido de vanadio (V_2O_5) en un rango de temperatura de 500°c and 600°C. Se caracterizó las muestras por Microscopía Electrónica de Barrido (SEM), Espectroscopía de Energía Dispersada (EDS) y Difracción de Rayos X (XRD) y se estudió la morfología, la composición y la estructura de las capas formadas en donde se observó una buena protección de la capa rociada térmicamente y que la mayor degradación del recubrimiento protector generalmente ocurrió a temperaturas superiores a las temperaturas de fusión de las sales, además la velocidad de corrosión aumenta con la temperatura y disminuye con el tiempo de exposición.

Palabras clave: aluminio; corrosión; alta temperatura; rociado térmico.

1. Introduction

Corrosion resistance at high temperatures is one of the main requirements for boosting boiler improvement because it increases oxidation in the boiler parts. Boilers undergo corrosion by molten salts, and the temperature leads to an increase in the oxygen diffusion through the molten salt film, causing a reaction in the active elements of the substrate and forming an oxide layer, a process that is amplified if molten salts are present in the corrosive environment. The behavior

How to cite: Pérez-Muñoz, D, Marulanda-Arévalo, J.L. and Tristancho-Reyes, J.L, Protection against corrosion by molten salts through aluminum coatings deposited by arc thermal spray on ASTM A53 grade B steel. DYNA, 87(213), pp. 22-27, April - June, 2020.

of carbon steel is not appropriate against corrosion by molten salts because these create porous oxide layers, which are easily removed and accelerate the corrosion process. These oxide layers also reduce heat transfer, drastically affecting the boiler's thermal efficiency. Hence, the coating of these materials is pivotal for increasing their corrosion resistance and their life span under these environments. In addition, these steel protective coatings will support steel works at 400 °C and 600 °C in thermal plants, thus increasing the thermal efficiency of the power generation process and lowering environmental pollution by pollutant gases such as CO_2, SO_2, and NO_x, as it would also reduce fossil fuel consumption [1-4].

ASTM A53 grade B steel is usually used as tubes, re-heater and over-heater in boilers, which use fossil fuel. This kind of fuel in Colombia content high percent of Vanadium, Sulfur and Sodium [5,6]; hence when they work at higher temperatures than 600 °C, they react with oxygen and become to convert into V_2O_5 and Na_2SO_4. The aforementioned information is the main reason for the selection of oxides in this research [6,7].

Arc thermal spray is a metallurgical process by which layers of the same material or other materials are added to a metal. The resulting combination may have better physical, mechanical, and chemical properties or lower costs than the uniform material. This process has advanced through the development of new alloys and processes, which are also highly endorsed in the industry, both in part manufacture and maintenance, thus expanding their application fields. Aluminum is frequently used for protective coatings because it forms an Al_2O_3 layer, which exhibits remarkable adherence to the substrate and excellent behavior against corrosion. In addition, as low alloy carbon steels possess low chromium content and other alloy elements that may contribute to improving their performance at high temperatures, they require a surface coating to improve their performance and for smooth operation [1,2,9-11].

Because of its low cost and high deposition rate, the arc thermal spray process is widely used to apply coatings to metals and alloys for protection against corrosion and wear [9,11]. However, the main problems presented by coating deposition by thermal spray are the porosity generated and presence of micro and macro cracks generated by the impact speed of the deposition particles when they reach the substrate and by the high cooling rate of the deposit as it reaches the substrate. Nevertheless, if all these variables are adequately controlled, it is very feasible to obtain low porosity coatings by arc thermal spray [12-18].

2. Experimental procedure

In this study, several 15 × 10 × 5 mm ASTM A53 grade B steel test cylinders, which are typically used in boilers, were manufactured. The chemical composition of the steel is given in Table 1. These test cylinders were subjected to a sanding process with emery paper No. 80, 200, 400, and 600 to produce homogeneous surfaces for corrosion tests and a good roughness profile, and thus secure proper adhesion of the coating applied by arc thermal spray. An Al coating was deposited on half of the test samples by electric arc thermal spray. This process was performed at a pressure of 55 psi and at a distance of 20-25 cm; the wire used was aluminum (99.5% pure) with a diameter of 2 mm and deposition flow rate of 2.7 kg/h at 100 A. After the deposition of the aluminum coating, test samples were exposed to heat treatment at 700 °C for 2 h to diffuse the Al throughout the substrate. Finally, the remaining samples were subjected to salt corrosion tests in the delivery state. After preparing all study samples, their weights were recorded to obtain initial comparative measurements.

Table 1.
ASTM A53 Grade B Steel chemical composition

C	Mn	P	S	Cu	Ni	Cr	Mo	V
0.3	1.2	0.05	0.045	0.4	0.4	0.4	0.15	0.08

Source: Adapted from Mohammad Najafi, PhD. Pipeline infrastructure Renewal and Asset Management. 2016

Figure 1. Samples placed in crucible
a) Crucible inside of Oven. b) Crucibles up-view
Source: The Authors, 2019.

Subsequently, corrosion tests were performed by covering all samples with a corrosive agent (80% V_2O_5 and 20% Na_2SO_4), which is a precursor of $Na_2OV_2O_45V_2O_5$ and $5Na_2OV_2O_411V_2O_5$ complex vanadates, [17-22]. In addition, they were exposed to 500 °C and 600 °C with extractions (2 test samples) at 1, 5, 10, 20, 50, and 100 h. After each extraction, the samples were weighed to track their mass variation and prepared according to ASTM E3 for their characterization by SEM and EDS. Fig. 1 shows the study samples placed in the crucible; in every single crucible one sample was placed, guaranteeing noncontact among them. In addition, each sample was full-covered by the corrosive agent.

3. Results and analysis

After measuring the test samples extracted during 100 h of the study at 500°C, the coated samples (CS) exhibited gradual mass increase during the first 20 h, but then showed

a decrease (mass loss) for the following 10 h before increasing slightly once again until reaching stability around −0.25 g. This behavior is due to the generation of surface oxides and their subsequent detachment, thus leading to the generation of substrate oxides [6,7,18,21]. This phenomenon can be observed between 20 and 100 h (see Fig. 2). On the other hand, the uncoated samples (US) experienced greater mass gain owing to the high generation speed of surface oxides, which easily detached after 20 h, suddenly transitioning from a mass gain of 1 g to a mass loss of approximately 2 g.

For the tests at 600 °C (Fig. 3), the behavior of the test samples was very similar to that of samples in the tests at 500 °C, with the major difference that the mass loss was greater and occurred in a shorter time (10 h), thus reporting a mass decrease of approximately 1.2 g for US. Likewise, the CS also experienced a mass decrease, reaching values close to those reported at 500 °C. Similarly, the CS managed to stabilize their mass by 100 h, which is a behavior related to the generation of surface oxides [19-26]. In both temperature tests, CS showed a clear mass increase after 20 h of exposure, caused by the generation of oxides, which (as indicated by the SEM images) are not necessarily aluminum oxides (coating), as coating loss is clearly visible after 30 h.

A surface analysis via SEM/EDS of the CS after 20 h at 500 °C is shown in Fig. 4, wherein remains of the solidified salts may be observed, as well as the presence of Al protective oxides, which prevent contact between the salts and substrate until the latter's oxidation time. The aforementioned is showed in EDS spectra, Fig. 5.

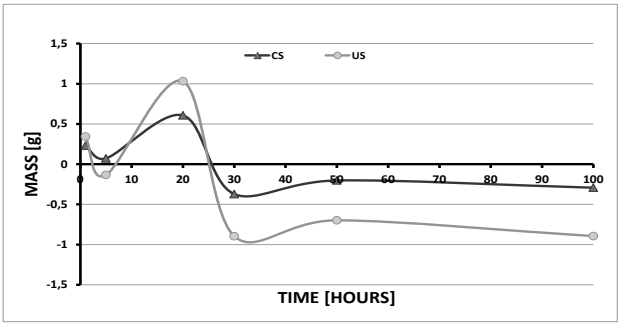

Figure 2. Mass Variation at 500 °C
Source: The Authors, 2019.

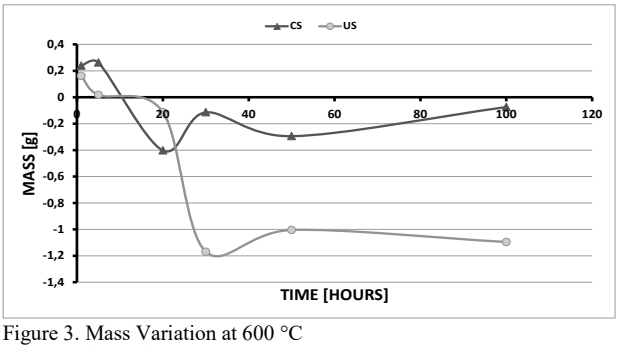

Figure 3. Mass Variation at 600 °C
Source: The Authors, 2019.

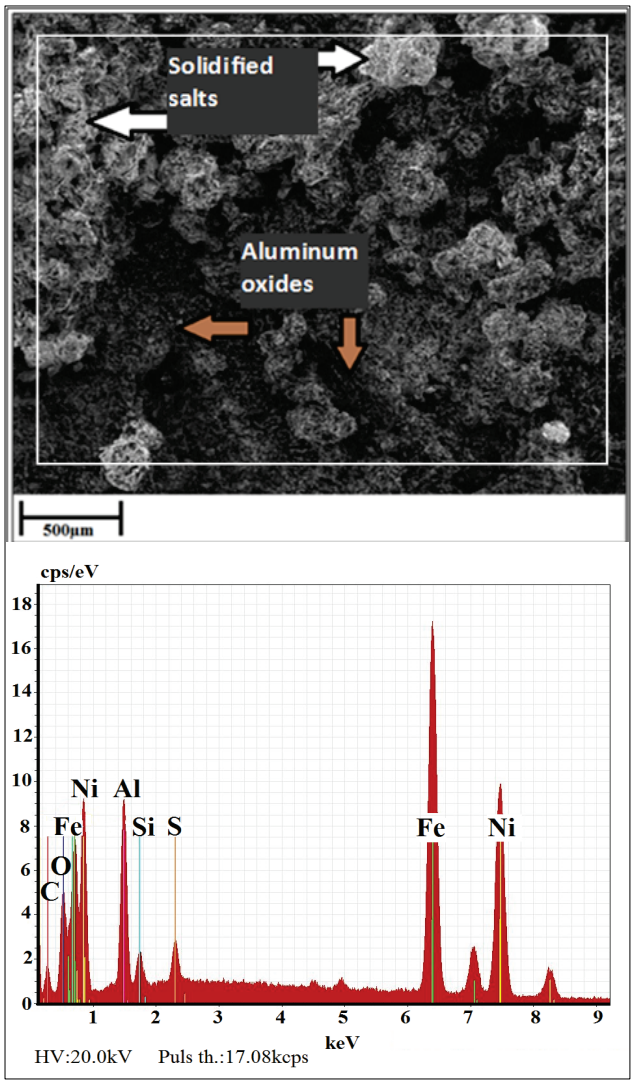

Figure 4. Superficial SEM/EDS image shows coating after 20 h at 500 °C
Source: The Authors, 2019.

Fig. 5 displays the cross section of a coated sample at a later time (30 h) for the same temperature (500 °C). Therein, the high porosity gained by the coating as well as the detachment of the aluminum layer and its oxides, thus leaving the initially deposited bond layer (nickel) exposed, may be observed. This information is in accordance with results of Villada, LeSung and Yang et al [5-7]. Likewise, the generation of iron oxides on the substrate and the detachment of the nickel layer from the steel are visible in this figure. These findings corroborate the behavior shown in Figs. 2 and 3, for which there are drastic mass gains and losses. Same phenomena was observed by Haiyan and Zhenhua [27-29].

Fig. 6 depicts the coated sample cross section after 50 h at 500 °C, in which the Al layer and its oxides have completely disappeared, leaving only the nickel layer. However, this nickel layer is not sufficient for insulating the substrate from the corrosive environment, since the generation of an iron oxide layer between the nickel and substrate is clearly seen.

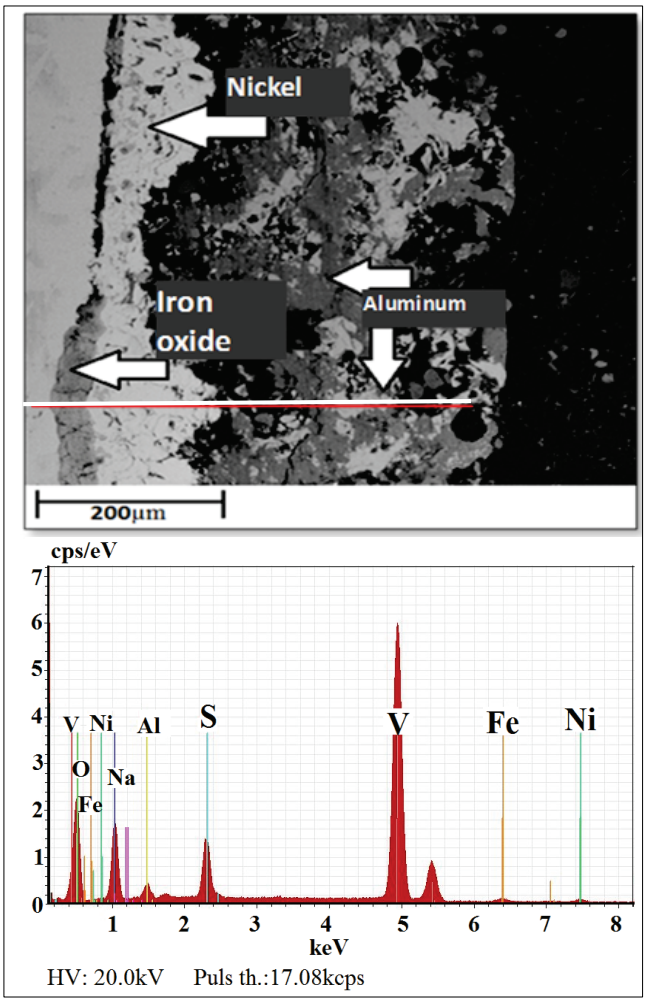

Figure 5. Coated sample cross section SEM/EDS image after 30 h at 500 °C
Source: The Authors, 2019.

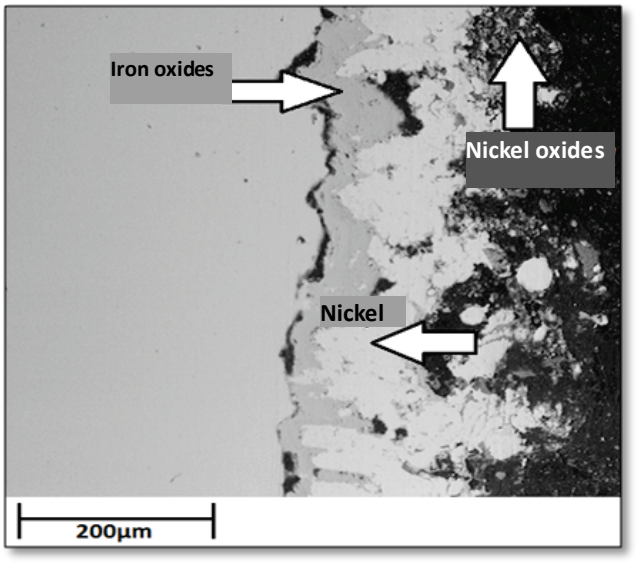

Figure 6. Coated sample cross section after 50 h at 500 °C
Source: The Authors, 2019.

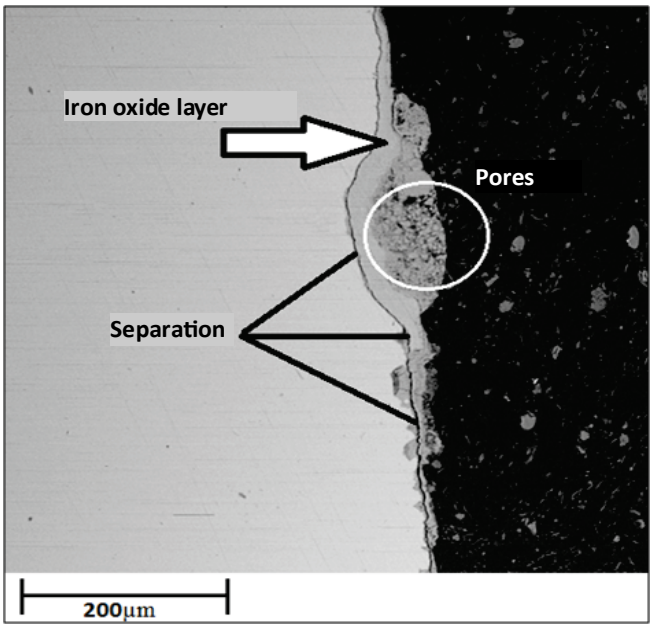

Figure 7. Cross sections of the coated samples after 100 h at 500 °C
Source: The Authors, 2019.

The presence of nickel oxides demonstrates the protection provided by the nickel layer against corrosion, since although the generation of iron oxides layers was facilitated by its high porosity levels, nickel continues to exhibit an affinity for oxygen, thus generating oxide layers that protect the substrate until they are totally detached [30-33].

The porosities presented both in the nickel and iron oxide layers will lead to their future detachment, which is consistent with the sudden mass loss observed in the study samples at both temperatures.

Finally, as expected, at a temperature of 500 °C for 100 h, the coating disappeared completely, leaving the substrate completely exposed to the corrosive environment (see Fig. 7). Therefore, only iron oxides will now be formed. However, these oxides exhibit poor adhesion owing to their high porosities, and separations are observed in the layer-substrate border, which means that their future detachment from the base material is imminent, represented in the notorious mass loss observed in Fig. 2 and Fig. 3.

4. Conclusions

- The aluminum coatings deposited by arc thermal spray on ASTM A53 grade B steel showed good protective behavior against corrosion from molten salts [18-20] (Sodium Persulfate+Vanadium Pentoxide) at 500 °C until 30 h because the aluminum layer forms oxides that prevent the substrate from coming into contact with molten salts, thus increasing their life span.
- The high porosities exhibited by the aluminum coating deposited by electric arc thermal spray, in addition to the aggressive corrosive environment created at 500 °C and molten salts (Sodium Persulfate+Vanadium Pentoxide),

led to the partial detachment of the aluminum protector coating [21-25] after 30 h, with total detachment at 50 h. However, at 600 °C, these phenomena occurred before partial detachment at 20 h and total detachment at 30 h.

- The nickel-bonding layer prevented efficient aluminum diffusion throughout the substrate, thus failing to reach the initial purpose of increasing the corrosion resistance of substrate against salts.

Acknowledgements

We appreciate the financial support received to carry out this research by the Office of Vice-president for Research, Innovation and Extension from Universidad Tecnológica de Pereira

References

[1] Marulanda, J.L. Tristancho J.L. y González. H.A., Rociado térmico. Universidad Tecnológica de Pereira. Pereira, Colombia, 2015.

[2] Muhamad, H.M., Nor-Hayati, S.K., Abas, N.R. and Noriyati, M.S., Performance and microstructure analysis of 99.5% aluminium coating by thermal arc spray technique. Procedia Engineering, 68, pp. 558-565, 2013. DOI: 10.1016/j.proeng.2013.12.221

[3] Venkateswararao, A., Sambasiva, R., Neeta, P., Kamaraj, M. and Ravi, S., Hot corrosion studies on Ni-base superalloy at 650 °C under marine-like environment conditions using three salt mixture (Na2SO4 + NaCl + NaVO3). Corrosion Science, 105 pp. 109-119, 2016. DOI: 10.1016/j.corsci.2016.01.008

[4] Reza, J. and Esmaeil, S., High-temperature corrosion performance of HVAF-sprayed NiCr, NiAl, and NiCrAlY coatings with alkali sulfate/chloride exposed to ambient air. Corrosion Science, 160, art. 108066, 2019. DOI: 10.1016/j.corsci.2019.06.021

[5] Carolina-Villada, A.B. and Thomas-Bauer, F.B., High-temperature stability of nitrate/nitrite molten salt mixtures under different atmospheres. Applied Energy, 226, pp. 107-115, 2018. DOI: 10.1016/j.apenergy.2018.05.101

[6] Le, S., Qian-Gang, F., Jia, S, and Guang-peng, Z., Comparison investigation of hot corrosion exposed to Na_2SO_4 salt and oxidation of $MoSi_2$ based coating on Nb alloy at 1000 °C. Surface and Coatings Technology. 385, Art. 125388, 2020. DOI: 10.1016.j.surfcoat.2020.125388

[7] Yang, W., Zhiming, B., Lei, Z., Wenting, H. and Hongbo, G., Hot corrosion behavior of $NdYbZr_2O_7$ exposed to V_2O_5 and Na_2SO_4 + V_2O_5 molten salts. Ceramic International, 2019. DOI: 10.1016/j.ceramint.2019.12.083

[8] Marulanda, J.L. Posada, B. y Gamboa, D. Protección contra la corrosión por sales fundidas de un acero al carbono por rociado térmico. Scientia et Technica, 1(36), pp. 485-490, Universidad Tecnológica de Pereira, 2007. DOI: 10.22517/23447214.5007

[9] Cinca, N., Camello, C. and Guilemany, J., An overview of intermetallics research and application: status of thermal spray coatings. Journal of Materials Research and Technology 2(1), pp. 75-86. 2013. DOI: 10.1016/j.jmrt.2013.03.013

[10] Bolot, R., Planche, M., Liao, H. and Coddet, C., A three-dimensional model of the wire-arc spray process and its experimental validation. Journal of Materials Processing Technology, 200(1-3), pp. 94-105, 2018. DOI: 10.1016/j.jmatprotec.2007.08.032

[11] Abd-Malek, M., Hayati-Saad, N., Kiyai-Abas, S., Nik-Roselina, N. and Moh-Shah, N., Performance and microstructure analysis of 99.5% aluminium coating by thermal arc spray technique. Procedia Engineering, 68, pp. 558-565, 2013. DOI: 10.1016/j.proeng.2013.12.221

[12] Trevisan, R. and Lima, C., Aspersao termica fundamentos e aplicacoes. Editorial Artliber, Sao Paulo, Brasil, 2002.

[13] Pombo, R., Paredes, R., Schereiner, H. and Calixto, A., Comparison of aluminum coatings deposited by flame spray and by electric arc spray. Surface and Coatings Technology, 202, pp. 172-179, 2011. DOI: 10.1016/j.surfcoat.2007.05.067

[14] Marulanda, J.L., Tristacho, J.L. y González. H., La tecnología de recuperación y protección contra el desgaste está en el rociado térmico. Revista Prospectiva, 12(1), pp. 70-78, 2014.

[15] Lortrakul, P., Trice, R.W., Trumble, K.P. and Dayananda, M.A., Investigation of the mechanisms of Type-II hot corrosion of superalloy CMSX-4. Corrosion Science, 80, pp. 408-415, 2014. DOI: 10.1016/j.corsci.2013.11.048

[16] Yan, Y.F., Xu, X.Q., Zhou, D.Q., Wang, H., Wu, Y., Liu, X.J. and Lu, Z.P., Hot corrosion behaviour and its mechanism of a new alumina-forming austenitic stainless steel in molten sodium sulphate. Corrosion Science, 77, pp. 202-209, 2013. DOI: 10.1016/j.corsci.2013.08.003

[17] Fan, Q.X., Jiang, S.M., Yu, H.J. and Gong, J., Microstructure and hot corrosion behaviors of two Co modified aluminide coatings on a Ni-based superalloy at 700 °C., Applied Surface Science, 311, pp. 214-223, 2014. DOI: 10.1016/j.apsusc.2014.05.043

[18] Schaefer, K. and Miszczyk, A., Improvement of electrochemical action of zinc-rich paints by addition of nanoparticulate zinc. Corrosion Science, 66, pp. 380-391, 2013. DOI: 10.1016/j.corsci.2012.10.004

[19] Ruiz-Cabañas, F.J., Prieto, C., Madina, V., Fernández, A.I. y Cabeza, L.F., TES-PS10 postmortem tests: carbon steel corrosion performance exposed to molten salts under relevant operation conditions and lessons learnt for commercial scale-up. Journal of Energy Storage, 26, art. 100922, 2019. DOI: 10.1016/j.est.2019.100922

[20] Han-Seung, L., Jitendra, S. and Park, J., Pore blocking characteristics of corrosion products formed on Aluminum coating produced by arc thermal metal spray process in 3.5 wt.% NaCl solution. Construction and Building Materials, 113, pp. 905-916, 2016. DOI: 10.1016/j.conbuildmat.2016.03.135

[21] Zhao, Z., Xiang, H., Dai, F-Z., Peng, Z. and Zhou, Y., On the potential of porous ZrP2O7 ceramics for thermal insulating and wave-transmitting applications at high temperatures. Journal of the European Ceramic Society, 40(3), pp. 789-797, 2020. DOI: 10.1016/j.jeurceramsoc.2019.11.016

[22] Li, H.Y, Duan, J.Y. and Wei, D.D., Comparation on corrosión behaviour of arc sprayed and zinc-rich coatings. Surfaces and Coatings Technology. 235 pp. 259-266, 2013. DOI: 10.1016/j.surfcoat.2013.07.046

[23] Gupta, M., Li, X.-H., Markocsan, N. and Kjellman, B., Design of high lifetime suspension plasma sprayed thermal barrier coatings. Journal of the European Ceramic Society, 40(3), pp. 768-779, 2020. DOI: 10.1016/j.jeurceramsoc.2019.10.061

[24] Ran, L., Zheng, Z,. Dingyong, H., Lidong, Z. and Xiaoyan, S., Microstructure and high-temperature oxidation behavior of wire-arc sprayed Fe-based coatings. Surface and Coatings Technology, 251, pp. 186-190, 2014. DOI: 10.1016/j.surfcoat.2014.04.024

[25] Hafiz, M., Saad, N. and Abas, N., Thermal arc spray overview. IOP Conf. Series: Materials Science and Engineering, 46. 2013.

[26] Baiamonte, L., Marra, F., Gazzola, S., Giovanetto, P., Bartuli, C., Valente, T. and Pulci. G., Thermal sprayed coatings for hot corrosion protection of exhaust valves in naval diesel engines. Surface and Coatings Technology, 295, pp. 78-87, 2016. DOI: 10.1016/j.surfcoat.2015.10.072

[27] El-Awadi, G., Abdel-Samad, S. and Ezzat, S., Hot corrosion behavior of Ni based Inconel 617 and Inconel 738 superalloys. Applied Surface Science, 378, pp. 224-230, 2016. DOI: 10.1016/j.apsusc.2016.03.181

[28] Salehnasab, B., Poursaeidi, E., Mortazavi, S. and Farokhian, G., Hot corrosion failure in the first stage nozzle of a gas turbine engine. Engineering Failure Analysis, 60, pp. 316-325, 2016. DOI: 10.1016/j.engfailanal.2015.11.057

[29] Haiyan, H., Zongjie, L., Wan, W. and Chungen, Z., Microstructure and hot corrosion behavior of Co-Si modified aluminide coating on nickel based superalloys. Corrosion Science, 100, pp. 466-473, 2015. DOI: 10.1016/j.corsci.2015.08.011

[30] Gheno, T., Zahiri, M., Arthur, H. and Gleeson, B., Reaction morphologies developed by nickel aluminides in type II hot corrosion conditions: the effect of chromium. Corrosion Science, 101, pp.32-46, 2015. DOI: 10.1016/j.corsci.2015.08.029

[31] Zhenhua, X., Dai, J., Niu, J., He, L., Mu, R. and Wang, Z., Isothermal oxidation and hot corrosion behaviors of diffusion aluminide coatings deposited by chemical vapor deposition. Journal of Alloys and Compounds, 637, pp. 343-349, 2015.
[32] Mukherjee, B., Islam, A., Pandey, K.K., Rahman, O.S.A., Kumar, R., Kumar-Keshri, A., Impermeable CeO_2 overlay for the protection of plasma sprayed YSZ thermal barrier coating from molten sulfate-vanadate salts. Surface and Coatings Technology, 358, pp. 235-346, 2019. DOI: 10.1016/j.surfcoat.2018.11.048
[33] Zhang, K., Zhang, T., Zhang, X. and Song, L., Corrosion resistance and interfacial morphologies of a high Nb-containing TiAl alloy with and without thermal barrier coatings in molten salts. Corrosion Science, 156, pp. 139-146, 2019. DOI: 10.1016/j.corsci.2019.05.011

D. Pérez-Muñoz, is BSc. Eng. in Mechanical Engineer in 2014, from the Universidad Tecnológica de Pereira, MSc. in Mechanical Engineering, focusing on advanced materials in 2017, working on corrosion, characterization, and nano-characterization of materials programs and projects, with emphasis on coatings, thin films, and microscopy at the Universidad Tecnológica de Pereira and SENA where he has published articles in scientific journals. He is currently a professor and researcher at the Faculty of Mechanical Engineering of the Universidad Tecnológica de Pereira, Pereira, Colombia.
ORCID: 0000-0001-5416-1633

J.L. Marulanda-Arévalo, is BSc. Eng in Metallurgical Engineer in 1999 from the Industrial University of Santander, MSc. in Metallurgical Engineering in 2002 from the Universidad Industrial de Santander, and Dr. in Advanced Chemistry in 2012 at the Universidad Complutense de Madrid. From 2003 to 2004, he worked on corrosion programs and projects; from 2005 to 2006, he worked on welding projects, and since 2006 he has been an associate professor in the Materials Department of the Faculty of Mechanical Engineering of the Universidad Tecnológica de Pereira. His research interests include coatings, corrosion characterization, welding, and tribology.
ORCID: 0000-0002-2607-3625

J.L. Tristancho Reyes, is BSc. Eng. in a Metallurgical Engineer in 1998, MSc. in Metallurgical Engineering in 2005 all of them from the Universidad Industrial de Santander, Colombia, and a Dr. of Materials Science in 2011 at the Centro de Investigación en Materiales Avanzados S.C. (CIMAV), Mexico. From 2002 to 2004 he worked on corrosion, physical metallurgy, and materials programs and projects; since 2005 he has been a full-time professor assigned to the Materials Department of the Faculty of Mechanical Engineering of the Universidad Tecnológica de Pereira, and currently Associate Professor and Coordinator of the Centro de Estudios y Consultoría en Ensayos No Destructivos y Resistencia de Materiales (CECEND) and Advanced Materials Research Group (GIMAV), Coordinator of the Universidad Tecnológica de Pereira. His research interests include coatings, material characterization, corrosion, welding, and tribology.
ORCID: 0000-0003-3550-8042